# Ab-initio Simulations of Higher Miller Index Si:$SiO_2$ Interfaces for FinFET and Nanowire Transistors

Hongfei Li[1], Yuzheng Guo[1], John Robertson[1] and Y Okuno[2].

1 Engineering Dept, Cambridge University, Cambridge, CB2 1PZ, UK

2 Taiwan Semiconductor Manufacturing Company (TSMC), Hsinchu Science Park, Taiwan

## Abstract

Models of three representative higher Miller index interfaces, Si(310):$SiO_2$, Si(410):$SiO_2$ and Si(331):$SiO_2$, have been built by an ab-initio molecular dynamics method. We show that each interface can be made as a fully bonded network without any defects and has a reasonable electronic structure for use in FinFETs (fin field effect transistors) or gate-all-around nanowire devices. The differences in numbers of oxygen bridges are attributed to the intermediate sub-oxide components and the atomic step structure. The interface bonding schemes to passivate different densities of dangling bonds on different facets are also analyzed.

Keywords: Si, higher index, interface, $SiO_2$, FinFET

## Introduction

The dominance of Si in microelectronics is largely based on the high quality of the interface between Si and its native oxide $SiO_2$, especially for the canonical Si(001), Si(110) and Si(111) facets, which have been thoroughly investigated [1-7]. With the growing demands for smaller devices, it is necessary to overcome factors such as the short channel effect [8] to continue scaling. This has led to the introduction of some novel three-dimensional device structures such as the FinFET, Tri-gate and gate all around (GAA) nanowire devices [9-11], in order to retain good electrostatic control of the channel. These non-planar devices however involve some higher Miller index facets of Si [12-16], such as the Si(n10) and Si(nn1) facets, due to the tapering of the fin sidewalls [17]. Therefore, the quality of these higher index interfaces could determine the final device performance [18,19]. Thus, a deeper understanding of higher index Si/$SiO_2$ interfaces is desirable.

Interfaces based on two general higher index Si facets, Si(n10) and Si(nn1), are good models for the appropriate Si:$SiO_2$ interfaces in the FinFET [13]. It is often noted that such interfaces keep the properties of simpler Si facets such as Si(001), Si(110) and Si(111), and the higher index Si surface atoms are often classified by their suboxide state or similarity to low-index surface atoms [12]. Si(001)-like atoms appear as $Si^{2+}$ on the surface, while both Si(110)-like and Si(111)-like atoms are $Si^{+}$, differing only in the direction of the dangling bonds. The XPS data of Ohno [13] confirm that the density of $Si^{2+}$ sites is less on higher index surfaces compared to Si(001) for various oxidation times. However, Ogata [12] noted that higher index facets should have more Si(001) facets based on the relative oxidation rates of Si(111)

and Si(001). On the other hand, Stesmans [15] found a nine times greater electron spin resonance (ESR) signal for Si(111)-like $P_b$ defects than for Si(001)-like defect sites.

The key question for the higher index interfaces is how does the 2.2 higher Si atom density in Si than in $SiO_2$ affect the ability of Si-O bonds to form at all sites across the interfaces. For the Si(111) or Si(011) case, each Si atom on the Si side has a single dangling bond, and this largely matches the dangling bond density on the $SiO_2$ side. On the other hand, a Si(001) face has two dangling bonds per interface atom, which is much more difficult to match with the $SiO_2$ side. A way to achieve the matching is for two dangling bonds on adjacent Si atoms on the Si side to form Si-O-Si bridges [20-24]. This ties off half of the dangling bonds, and allows the remaining dangling bonds to then to bond across the interface. A similar process is that adjacent Si dangling bonds could form Si-Si dimers [25,26]. On higher index surfaces, the question is whether the presence of narrow terraces, steps or other factors will interfere with the bridge forming or dimerisation process.

The 2.2 fold increase in volume from Si to $SiO_2$ during thermal oxidation is also a source of stress. Stesmans [27] has noted that dangling bond defects ($P_b$ centers) can be thought of as mismatch defects between the Si side and the $SiO_2$ side. This possibility can occur for Si oxidised under a high dielectric constant $HfO_2$ layer [28] on FinFETs or on GAA nanowires.

Another way to terminate a Si(100) surface would be with Si(111) facets [25]. These would protrude into the $SiO_2$ and form a thicker, more graded interface rather than an abrupt one [25,26]. However, such a graded interface might show lower reliability. Overall, there are few results which show how the dangling bonds on the Si side of higher index interfaces become passivated.

Here, we investigate thoroughly the three different higher index interfaces, Si(310):$SiO_2$, Si(410):$SiO_2$ and Si(331):$SiO_2$ by ab-initio methods, to derive the interfacial atomic structures and their electronic properties. It is found that all these three interfaces can be built without any defects and are thus suitable for FinFETs. Their electronic properties are further analysed to understand the difference in local surface structure. A real FinFET model involving Si(310):$SiO_2$ and Si(001):$SiO_2$ interfaces is also built to prove the practicability in a FinFET device.

**Methods**

Our simulations use the density functional theory, plane-wave pseudopotential method as implemented in the CASTEP code [29]. The generalised gradient approximation (GGA) exchange correlation functional and the ultrasoft pseudopotentials with a cutoff energy 380 eV were used in the molecular dynamics (MD) and geometry optimizations. For k-point sampling, we took the Monkhorst-Pack (MP) scheme with 3×3×1, 3×2×1, and 2×1×1 k-point mesh for the MD and geometry tasks of Si(310):$SiO_2$, Si(410):$SiO_2$, and Si(331):$SiO_2$ interfaces respectively.

The interface models were built according to the following steps. First, a Si high index surface slab model (thickness over 8 Å) was cleaved from the Si bulk structure. Secondly, a

larger supercell of this Si high index surface slab model was chosen to attach to the $SiO_2$ surface slab model. Thirdly, some extra O atoms were inserted where necessary to form oxygen bridges to connect dangling bonds on Si(100)-like regions. The distance and the relative position of the two slabs were then adjusted to allow interface bonds to form. In each supercell, a vacuum layer of 14 Å was included to suppress the interaction between the stack and its periodic image. The top and bottom Si and $SiO_2$ surfaces next to the vacuum were passivated by H atoms. The interface model was then given a high temperature MD anneal (1000 to 3000 K according to the model) for 2 ps to generate the amorphous $SiO_2$ layer, and then gradually cooled down to 300 K at a quenching rate of 100 K/ps. Finally, a geometry optimization was carried out until the residual force on each atom was smaller than 0.03 eV/ Å. We ensure each Si is 4-fold and each O is 2-fold so that no interface defects appear.

**Results**

Our three Si:$SiO_2$ interface models are shown in Figure 1. For the Si(310):$SiO_2$ model, we used a five atomic layer Si slab with five layers of amorphous $SiO_2$ on the top, containing 78 atoms in total in a 5.4 Å×8.6 Å×40.8Å orthorhombic supercell. The Si(410):$SiO_2$ model was constructed by five layers of Si and four layers of amorphous $SiO_2$, including 75 atoms in a 5.4 Å×11.5 Å×30.6 Å monoclinic supercell. We constructed the Si(331):$SiO_2$ interface with four layers of Si and four layers of $SiO_2$, which involves 162 atoms in a 7.7 Å×16.7 Å×39.0 Å orthorhombic supercell. Each of these three models is over 17 Å thick to suppress the top and the bottom surface's influence on the interface. The three bottom layer Si atoms in each model are fixed at their positions as in the bulk.

The Si(310):$SiO_2$ interface model is shown in Figure 1(a). The original Si(310) surface is sawtooth-like and has a single atomic step. Half of the surface Si atoms are Si(110)-like with one dangling bond, while the other half are Si(100)-like with two dangling bonds. MD results show that after oxidation, these dangling bonds are well passivated at the Si(310):$SiO_2$ interface, forming $Si^{+}$ and $Si^{2+}$ sub-oxide sites. The $Si^{2+}$ suboxide atoms lie closer to the $SiO_2$ side, whereas the $Si^{1+}$ suboxide atoms lie closer to the Si side, but still within the same atomic layer as $Si^{2+}$. $Si^{3+}$ sites do not appear in this model. The $Si^{2+}$ sites are largely at Si-O-Si bridges. We note that while Chadi [30] found that (100)Si vicinal surfaces favoured di-atomic steps, the equivalent (n10) interfaces can be made with single atomic steps.

The partial density of states (DOS) of the Si(310):$SiO_2$ interface is shown in Figure 2. The band gap of the whole interface structure is determined by the Si band gap due to the large band gap of $SiO_2$. The band gap for this model is 1.4eV within GGA, slightly larger than the experimental value of bulk Si, due to the quantum confinement effect in the slab model. The interface model has a clean band gap with no defect gap states. The band offset between the Si layers and $SiO_2$ layers is quite large for both conduction band (CB) and valence band (VB). We also calculate the partial DOS on Si of the different sub-oxide states. The partial DOS on the $Si^{+}$ and $Si^{2+}$ sites at the interface is quite similar to that on $Si^{0}$ (or bulk Si) due to the existence of Si-Si bonds, whereas the partial DOS on the $Si^{4+}$ sites has a much larger gap since these atoms belong to the $SiO_2$ layer. The electronic orbitals of Si valence band maximum (VBM) and conduction band maximum (CBM) shown in Figure 3 are both

delocalized throughout the Si layer, which is consistent with the partial DOS analysis. The CB orbital is slightly more localised towards the cell boundary in Fig 3(b), due to its preference to lie on $Si^{1+}$ sites.

The Si(410):$SiO_2$ interface model is shown in Figure 1(b). The original sawtooth-like Si(410) surface is well passivated by the $SiO_2$, just like the Si(310):$SiO_2$ interface discussed above. Both the $Si^+$ and $Si^{2+}$ suboxide sites appear in the model while $Si^{3+}$ does not appear. The difference to the (311) interface is that some Si-O-Si bridges passivate the extra dangling bonds on the Si surface atoms.

The electronic properties of the Si(410):$SiO_2$ interface is similar to Si(310):$SiO_2$ interface. We find a band gap of 1.7eV as contributed by the Si layer, and a large VB offset between Si and $SiO_2$ but somehow a smaller CB offset, as shown in Figure 4. The band gap is clean without any defect states. Partial DOS analysis based on different suboxide states show a similar behaviour for $Si^0$, $Si^+$ and $Si^{2+}$. The CBM and VBM orbitals are delocalized across Si layers as shown in Figure 5.

The Si(331) surface shows a armchair like structure and each of the Si atoms exposed at this surface has only one dangling bond. Therefore, no O bridges appear in the Si(331):$SiO_2$ interface and neither $Si^{2+}$ nor $Si^{3+}$ suboxide sites appear either. The $SiO_2$ part still shows a much larger band gap compared to the Si layers, and a large band offset is found between the Si and $SiO_2$ for both CB and VB, as shown in Figure 6. Some small peaks are found in the PDOS of $Si^{4+}$ sites in the $SiO_2$ band gap area, which is attributed to the attenuation of Si states into the $SiO_2$ layers. The CBM and VBM orbitals of the interface model in Figure 7 confirm this analysis.

We have also made a model of a real FinFET involving a horizontal Si(310):$SiO_2$ interface and a vertical Si(001):$SiO_2$ interface, on the basis of the above results, as shown in Figure 8. The simulation shows that both interfaces are quite sharp, within one or two atomic layers thick. The intersection of the two interfaces is still fully passivated, with no dangling bond defects. The partial DOS analysis of this model is quite similar to Figure 2. Thus the presence of the intersection does not degrade the overall quality of the Si(310):$SiO_2$ interface.

**Discussion:**

Both of the sawtooth-like surfaces, Si(310) and Si(410), consist of Si(100) and Si(110) partial facets. Moreover, in both interfaces $Si^+$ and $Si^{2+}$ stay in the same region within one atomic layer, and this is similar to the configuration of Si(100):$SiO_2$ interfaces found by the XPS data [13]. However, the Si(310) surface contains only one atomic step, while the Si(410) surface contains 3 atomic steps. The ratio of suboxide states is also different. On the Si(310) surface, half of the surface Si atoms are Si(110)-like ($Si^+$) and the other half are Si(100)-like ($Si^{2+}$). On Si(410), 40% of the surface Si atoms are Si(110)-like and the other 60% of surface atoms are Si(100)-like. Since the Si(410) surface have a larger portion of Si(100)-like atoms, this surface exposes more dangling bonds than Si(310). Therefore, it is more likely to form oxygen bridges on Si(410):$SiO_2$ interface to passivate the extra dangling bonds. This analysis

is consistent with our MD results that oxygen bridges form on Si(410) but less on Si(310) interfaces.

The armchair-like Si(331) surface consists of Si(110) and Si(111) partial facets, with only one atomic step. One third of surface Si atoms are Si(111)-like and the other two thirds are Si(110)-like atoms. Since both kinds of surface Si atoms here are $Si^{+}$ suboxide, it is as expected that $Si^{2+}$, $Si^{3+}$ and oxygen bridges do not appear at the relevant interface.

The PDOS on the $Si^{+}$ and $Si^{2+}$ sites are nearly identical in the VB energy range, but $Si^{2+}$ atoms make a larger contribution than $Si^{+}$ in the CB range. The PDOS of $SiO_2$ (or $Si^{4+}$) has a much larger band gap than Si for all three higher index interfaces, with a VB offset of 2.5eV. However the CB offset in Si(410):$SiO_2$ interface is much smaller than the other two interfaces. This difference results from the fact that Si(410) surface has three atomic steps which makes the surface morphology more disordered. Thus, the $SiO_2$ part in Si(410):$SiO_2$ interface is more disordered and its conduction band will tail further towards the Si band gap which makes the CB offset smaller.

The band gap of the Si slab is increased by quantum confinement from about 0.59 eV for bulk Si in GGA to about 0.87 eV for 7 layers of Si(111) in a supercell with only Si and $SiO_2$ components. However, there is a larger increase in Si band gap when as here we include a vacuum layer at the other interface, and that is why the observed Si band gaps in Fig 2 are quite large.

It is also interesting to understand these interface structures from the view of dangling bond density at truncated the Si surfaces and how these dangling bonds get passivated. We have calculated the dangling bond density on cleaved Si(310), (410), (331), (100), (110), (111) surfaces, as shown in Table 1. Both Si(310) and (410) surfaces have a dangling bond density slightly smaller than the Si(100) surface, while the dangling bond density of the Si(331) surface falls between the value of the Si(110) and the Si(111) surfaces which naturally match with $SiO_2$. Our MD results show that the extra dangling bonds on Si(410) surface are passivated by oxygen bridges. For the Si(310):$SiO_2$ interface, we find that both the first and the second layers of Si atoms in $SiO_2$ form oxygen bonding with Si surface atoms to passivate the dangling bonds.

Finally, we consider the interface energetics and how this compares to the energetics of Si surfaces. It is known from the work of Chadi and others [30-32] that the surface reconstructions of low index facets is driven by dangling bond minimisation (due to the cost of ~ 1.2 eV per dangling bond). We have carried out some calculations of interface energies for Si/$SiO_2$ for a few cases. We conclude that the interfacial energies are controlled by the energy penalty concept of Hamann, Bongiorno and Pasquarello [33]. For a given number of Si-Si and Si-O bonds, it costs slightly more (~0.5 eV) if these bonds occur as $Si^{1+}$ or $Si^{2+}$ sites than as only $Si^{0}$ and $Si^{4+}$ sites. Thus, an interface with Si(111)-like, Si(110)-like or Si(100)-like facets with Si-O-Si dimers would have a low energy, and not so dependent on the actual facet concerned.

How do these results affect the $P_b$ density in real devices? After the Si:$SiO_2$ interface is formed, it is subjected to an anneal in $H_2$ which tends to passivate most remaining $P_b$ centers. However, if the original $P_b$ centers are strained or consist of Ge, then the higher energy of these sites affects the dynamic equilibrium of H passivation and depassivation [34,16], resulting in a less effective net passivation of the initial $P_b$ sites. Thus, strained interfaces still show more $P_b$ sites. The fact that we can form fully passivated high index interfaces in our models suggests that many high index interfaces can be passivated afterwards by H annealing. However, it is clear that some higher index facets found on oxidised Si nanowires are too strained to easily passivate [16].

**Conclusion:**

We have investigated three high index interfaces, Si(310):$SiO_2$, Si(410):$SiO_2$ and Si(331):$SiO_2$. Our simulation results show that these interfaces could be made without any defects. Both the Si(310) and Si(410) surfaces contain $Si^+$ and $Si^{2+}$ suboxide atoms, while Si(331) contains only $Si^+$ atoms. The Si(410):$SiO_2$ interface involves oxygen bridges to passivate extra Si dangling bonds and the CB offset is small which has been attributed to the suboxide components and atomic step structure. The Si(310):$SiO_2$ interface has an additional layer of Si, forming Si-O-Si bonding as well to passivate additional Si dangling bonds. A real FinFET model involving Si(310):$SiO_2$ and Si(001):$SiO_2$ interfaces is built to further prove that the interface junction does not deteriorate each other.

References


1. T Hori, 'Gate Dielectrics and MOS ULSIs', Springer (1997)
2. E Arnold, J Ladell, G Abowitz, App Phys Lett 13 413 (1968)
3. T. Hattori and T. Suzuki, Appl Phys Lett **43**, 470 (1983).
4. F. J. Grunthaner, P. J. Grunthaner, R. P. Vasquez, B. F. Lewis, J. Maserjian, and A. Madhukar, Phys Rev Lett **43**, 1683 (1979).
5. F. J. Himpsel, F. R. McFeely, A. Talebibrahimi, J. A. Yarmoff, and G. Hollinger, Phys Rev B **38**, 6084 (1988).
6. E. H. Poindexter, G J Gerardi, M E Rueckel, P. J. Caplan, N M Johnson, D K Bieglsen, J Appl Phys **56**, 2844 (1984).
7. M L Green, E P Gusev, R Degraeve, E L Garfunkel, J App Phys 90 2057 (2001)
8. K. K. Young, IEEE Trans Electron Dev **36**, 399 (1989)
9. D. Hisamoto, W C Lee, J Kedzierski, H Takeuchi, K Asano, C Kuo, E Anderson, T J King, J Bokor, C Hu, IEEE Trans Electron Dev **47**, 2320 (2000).
10. B. S. Doyle, S Datta, R Chau, IEEE Electron Device Lett **24**, 263 (2003).
11. K J Kuhn et al, Tech Digest IEDM (2102) p8.01; K J Kuhn, VLSI-TSA (IEEE, 2011)
12. S. Ogata, S. Ohno, M. Tanaka, T. Mori, T. Horikawa, T. Yasuda, Appl Phys Lett **98**, 092906 (2011).
13. S. Y. Ohno, K Inoue, M Moritomo, S Arae, H Toyoshima, A Yoshigoe, Y Teraoka, S Ogata, T Yasuda, M Tanaka, Surf Sci **606**, 1685 (2012).
14. S Abe, D Ohno, R Kanemura, A Yoshigoe, Y Teraoka, S Ogata, T Yasuda, M Tanaka, App Phys Express 6 115701 (2013)
15. S. Iacovo, A. Stesmans, Appl Phys Lett **105**, 262101 (2014).
16. M Kivanescu, A Stesmans, R Kurstjens, EuroPhys Letts 106 66003 (2014)
17. C Auth et al, Tech Digest VLSI Technol (IEEE, 2012) T15.02
18. M Cho, R Ritzenthaler, R Krom, Y Higuchi, B Kaczer, T Chiarella, G Boccardi, M Togo, N Horiguchi, T Kauerauf, G Groeseneken, IEEE EDL **34** 1211 (2013)
19. T. H. Hsu, H. T. Lue, Y. C. King, Y. H. Hsiao, S. C. Lai, K. Y. Hsieh, R. Liu, C. Y. Lu, IEEE Trans Electron Dev **56**, 1235 (2009).
20. A. Pasquarello, M. S. Hybertsen, and R. Car, Nature **396**, 58 (1998).
21. A A Demkov, O F Sankey, Phys Rev Lett 83 2038 (1999)
22. R Buczko, S J Pennycook, S T Pantelides, Phys Rev Lett 84 943 (2000)
23. Y. Tu and J. Tersoff, Phys Rev Lett **84**, 4393 (2000).
24. Y. Tu and J. Tersoff, Phys Rev Lett **89**, 086102 (2002).
25. I. Ohdomari, H. Akatsu, Y. Yamakoshi, and K. Kishimoto, J Appl Phys **62**, 3751 (1987).
26. J. H. Oh, H. W. Yeom, Y. Hagimoto, K. Ono, M. Oshima, N. Hirashita, M. Nywa, A. Toriumi, and A. Kakizaki, Phys Rev B **63**, 205310 (2001).
27. A Stesmans, Phys Rev B 48 2418 (1993); Phys Rev Lett 70 1723 (1993)
28. M M Frank, E A Cartier, T Ando, S W Redell, J Bruley, Y Zhu, V Narayanan, ECS Solid State Letts 2 N8 (2013)
29. S. J. Clark, M. D. Segall, C. J. Pickard, P. J. Hasnip, M. J. Probert, K. Refson, and M. C. Payne, Z Kristallogr **220**, 567 (2005)
30. D. J. Chadi, Phys Rev Lett **59**, 1691 (1987); Surface Sci 299 311 (1994); D J Chadi, J R Chelikowsky, Phys Rev B 24 4892 (1981)
31. D. J. Chadi, Phys Rev B **29**, 785 (1984)
32. K Takayanagi, Y Tanishiro, M Takahashi, S Takahashi, J Vac Sci Technol A 3 1502 (1985)
33. D R Hamann, Phys Rev B 61 9899 (2000); A Bongiorno, A Pasquarello, Phys Rev B 62 16326 (2000)
34. A Stesmans, T Nguyen, V V Afanasev, J App Phys **116** 044501 (2014)

Table 1 Dangling bond density of cleaved Si(310), (410), (331), (100), (110), (111) surfaces.

| Si Surface | $Si^{+}$ | $Si^{2+}$ | Dangling Bonds | Area ($Å^{2}$) | DB/area ($Å^{-2}$) |
|---|---|---|---|---|---|
| (310) | 2 | 2 | 6 | 46.63 | 0.129 |
| (410) | 2 | 3 | 8 | 60.80 | 0.132 |
| (331) | 3 | 0 | 3 | 32.14 | 0.093 |
| (100) | 0 | 1 | 2 | 14.75 | 0.136 |
| (110) | 2 | 0 | 2 | 20.85 | 0.096 |
| (111) | 1 | 0 | 1 | 12.77 | 0.078 |

The item $Si^{+}$, $Si^{2+}$, dangling bonds, area in the table denote the number of $Si^{+}$, $Si^{2+}$ atoms, dangling bonds, and surface area of the relative Si surface unit cell. DB/area denotes the dangling bond density calculated from these values. There are no $Si^{3+}$ atoms on these cleaved Si surfaces.

Figure Captions

1. Unit cells of the atomic structure of (a) Si(310):$SiO_2$ interface; (b) Si(410):$SiO_2$ interface; (c) Si(331):$SiO_2$ interface.

2. The partial density of states of the Si(310):$SiO_2$ interface. (a) Partial DOS analysis based on different layer of the interface; (b) partial DOS analysis based on different sub-oxide state of Si.

3. The electronic orbital of (a) valence band maximum and (b) conduction band minimum for Si(310):$SiO_2$ interface.

4. The partial density of states of the Si(410):$SiO_2$ interface. (a) Partial DOS analysis based on different layer of the interface; (b) partial DOS analysis based on different sub-oxide state of Si.

5. The electronic orbital of (a) valence band maximum and (b) conduction band minimum for the Si(410):$SiO_2$ interface.

6. The partial density of states of the Si(331):$SiO_2$ interface. (a) Partial DOS analysis based on different layer of the interface; (b) partial DOS analysis based on different sub-oxide state of Si.

7. The electronic orbital of (a) valence band maximum and (b) conduction band minimum for the Si(331):$SiO_2$ interface.

8. An atomic model of a FinFET corner that involves Si(310):$SiO_2$ interface and Si(001):$SiO_2$ interface (a) atomic structure and (b) PDOS.

(a) (310) interface

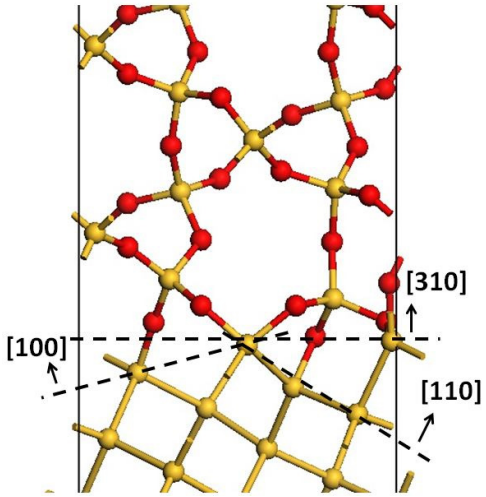


(b) (410) interface

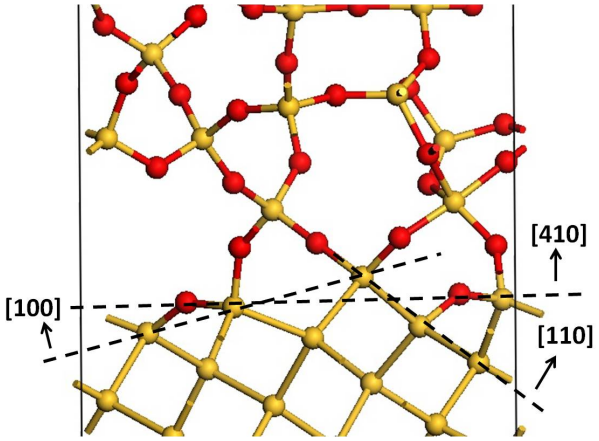


(c) (311) interface

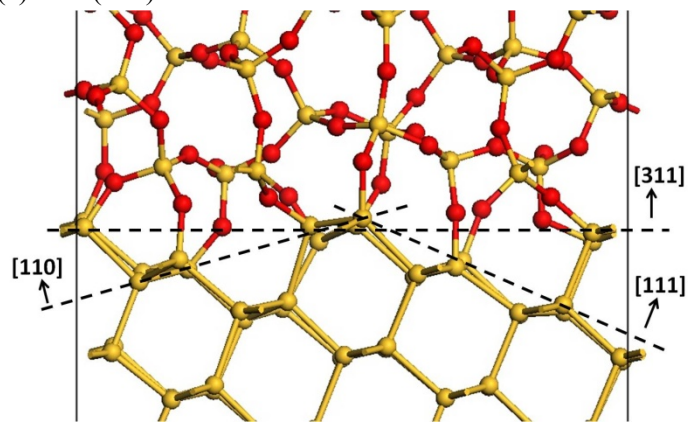


Figure 1.

(a) (b)

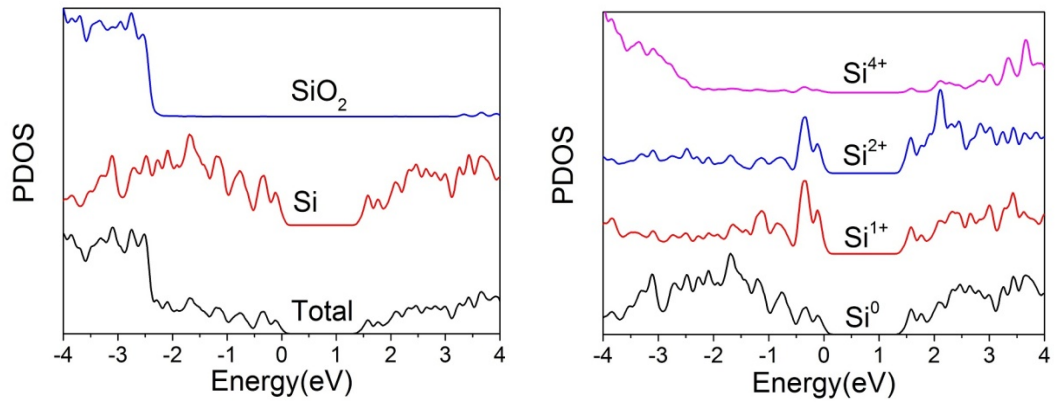
PDOS
SiO2
Si
Total
-4 -3 -2 -1 0 1 2 3 4
Energy(eV)
PDOS
Si4+
Si2+
Si1+
Si0
-4 -3 -2 -1 0 1 2 3 4
Energy(eV)

Figure 2.

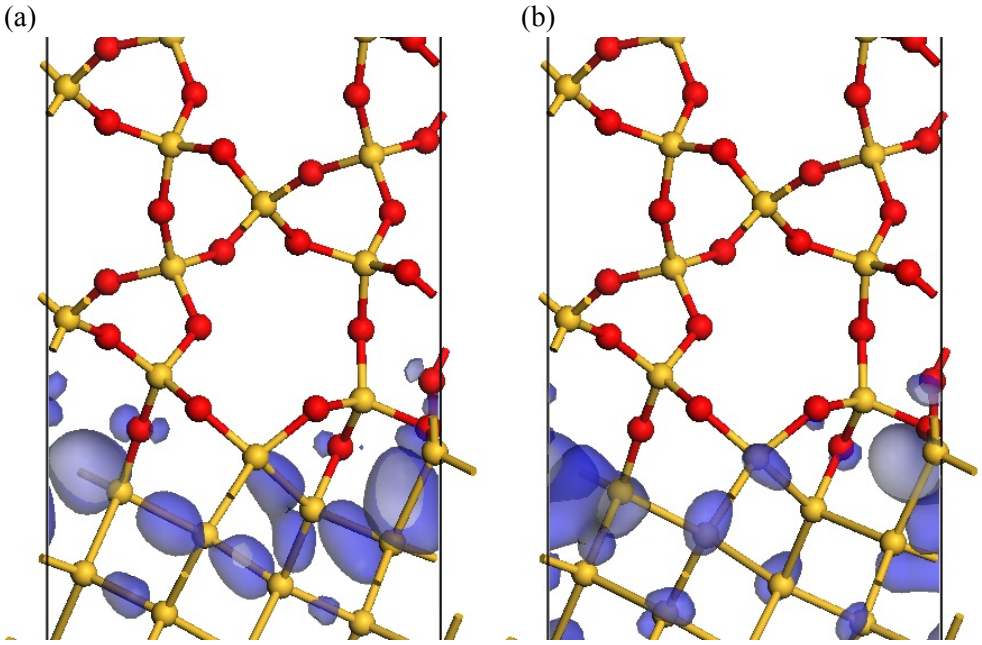


Figure 3.

(a)

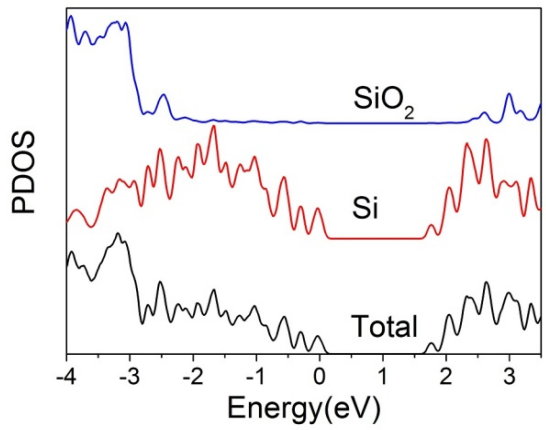
PDOS
SiO2
Si
Total
-4
-3
-2
-1
0
1
2
3
Energy(eV)

(b)

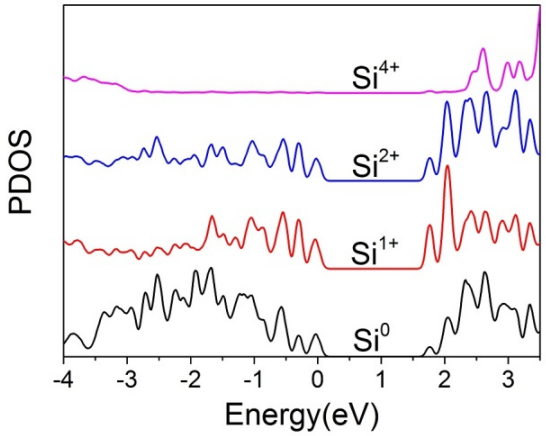
PDOS
Si4+
Si2+
Si1+
Si0
-4
-3
-2
-1
0
1
2
3
Energy(eV)

Figure 4.

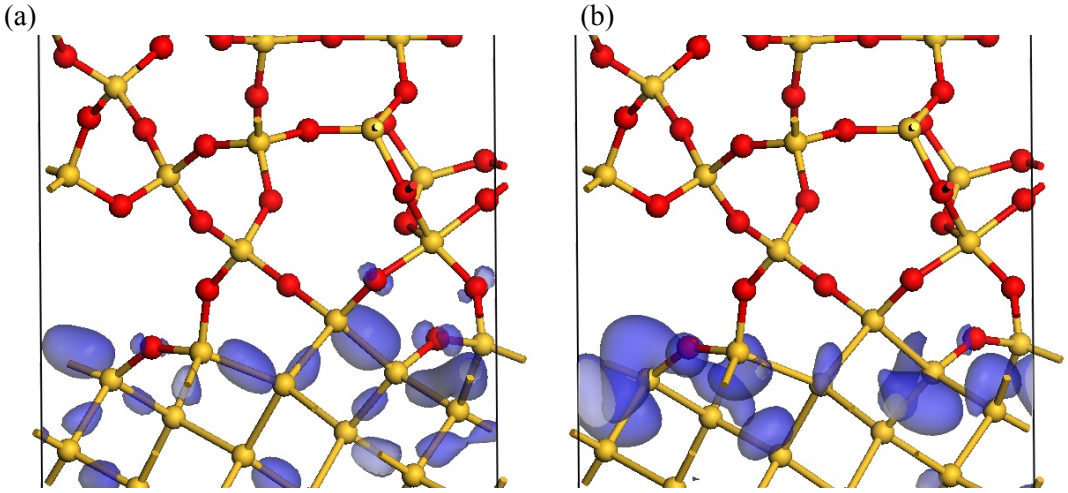


Figure 5.

(a) (b)

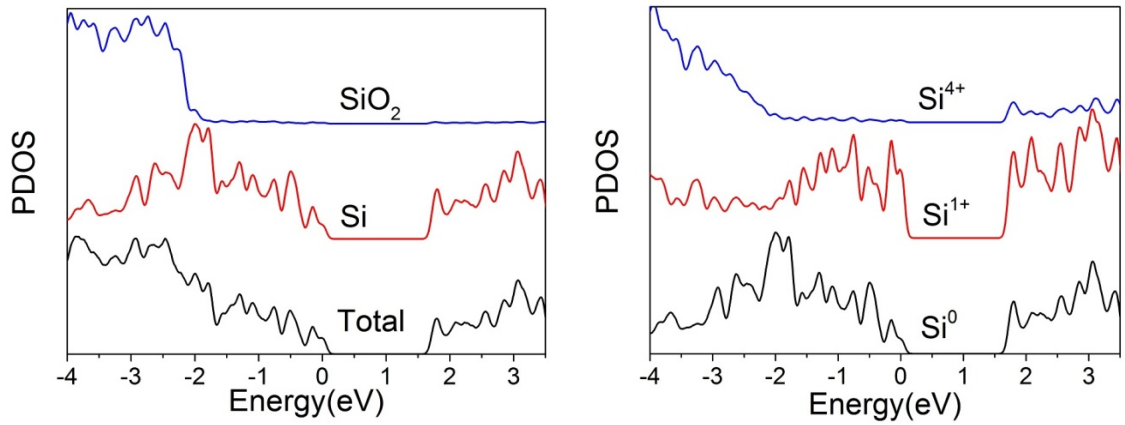
PDOS
SiO2
Si
Total
-4 -3 -2 -1 0 1 2 3
Energy(eV)
PDOS
Si4+
Si1+
Si0
-4 -3 -2 -1 0 1 2 3
Energy(eV)

Figure 6 .

(a) (b)

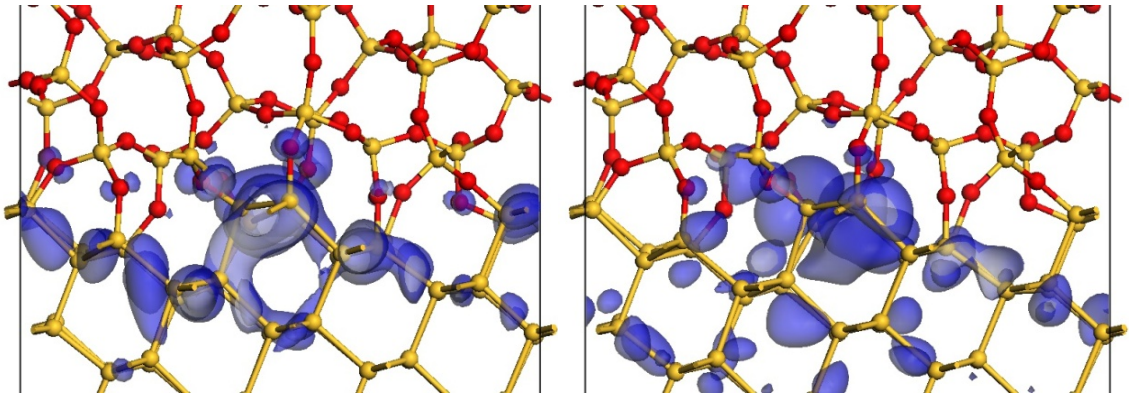

Figure 7.

(a) (b)

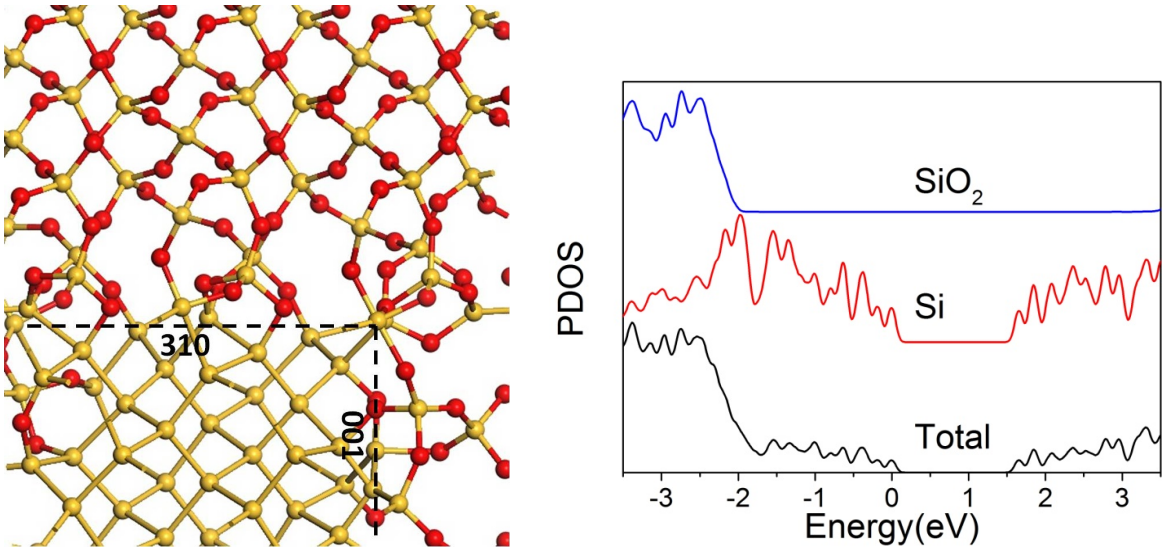


Figure 8.